Contents lists available at ScienceDirect

Physica C

Negative magnetoresistance slope in superconducting granular films

Boris Ya. Shapiro *, Irina Shapiro, Daniel Levi, Avner Shaulov, Yosef Yeshurun

Department of Physics, Institute of Superconductivity, Institute of Nanotechnology and Advanced Materials, Bar-Ilan University, Ramat-Gan 52900, Israel

ARTICLE INFO

ABSTRACT

A phenomenological theory is developed to explain the recently observed negative magnetoresistance slope in ultra-thin granular YBa$_2$Cu$_2$O$_{7-\delta}$ films. Viewing this system as a two-dimensional array of extended Josephson junctions, we numerically solve the sine-Gordon equations including a viscosity term that increases linearly with the external field. The solution yields a negative magnetoresistance slope setting in at a field that is determined by the geometry and thus independent of temperature, in agreement with the experimental results.

© 2014 Elsevier B.V. All rights reserved.

1. Introduction

Type-II superconductors may exhibit finite electrical resistance when exposed to external magnetic field. This magnetoresistance is associated with energy dissipating vortex motion driven by the current-induced Lorenz force. Usually, the magnetoresistance increases monotonically with the applied magnetic field, as the increased number of vortices causes larger energy dissipation. However, recently it has been demonstrated that superconducting systems may exhibit negative magnetoresistance slope, dR/dH, at high fields. For example, Morozov et al. [1] observed negative dR/dH in ultra-high fields (tens of Tesla) in Bi$_2$Sr$_2$CaCu$_2$O$_{8+d}$ (BSCCO) crystals, ascribing it to the interplay between tunneling of Cooper pairs and of quasiparticles in gaped and gapless regions, respectively [1,2]. Negative magnetoresistance slope in the Tesla regime was also observed in tungsten-based nanowire and superconducting ultrathin TiN networks by Cordoba et al. [3], ascribing it to the confined geometry in which the magneto-transport properties at high fields are strongly affected by surface superconductivity. The present theoretical work was motivated by the observation of negative magnetoresistance slope in ultrathin YBa$_2$Cu$_2$O$_{7-\delta}$ (YBCO) granular bridges in the low temperature region ($T < 40$ K), setting in at ~2 T independent of temperatures [4]. The previous explanations [1,3] cannot be applied directly for the granular YBCO system for the following reasons. The theory of Morozov et al. applies to the c-axis conductivity in BSCCO through gapless regions; the conductivity in the YBCO bridges is in the a–b plane where such conductivity is not feasible. Also, in Morozov et al. theory, the number of the quasi-particles in the

layers increases as a result of suppression of the superconducting gap and thus significant only at ultra-high fields. Moreover, this theory cannot explain the temperature-independent field for which the crossover to negative magnetoresistance is found. Also the theory proposed by Cordoba et al. cannot be applied directly to our granular film as it was designed for homogenous films. In this paper we propose a different model, appropriate for a granular material. Viewing the granular system as a two-dimensional array of extended Josephson junctions, we numerically solve the sine-Gordon equation including a viscosity term that increases linearly with the external field. This term reflects the increase in the number of quasi-particles as the number of vortices in the grains increases. The results of these calculations reveal negative magnetoresistance slope at high fields setting at a temperature-independent field, in agreement with the experimental results obtained in the ultra-thin granular YBCO films [4].

2. Model and basic equations

We consider superconducting grains orderly arranged in the x–z plane, forming a two-dimensional array of extended Josephson junctions. We neglect inhomogeneities in the x-direction and consider the system as alternating superconducting/dielectric in the z-direction with anisotropic ratio $\gamma = \lambda_z/\lambda_{xy}$, where λ_z is the penetration depth for currents along the z axis (perpendicular to the layers), and λ_{xy} is the penetration depth for currents in the plane parallel to the layers. An external field, H, is applied parallel to the layers (along the y-direction) and dc bias current, I, is flowing along the z-direction, as shown in Fig. 1. The magnetic field penetrates the inter-grain channels via the chains of Josephson vortices (JV), while Abrikosov vortices (AV) nucleate inside the grains as illustrated in the inset to Fig. 1. The sine-Gordon equation relating

* Corresponding author.
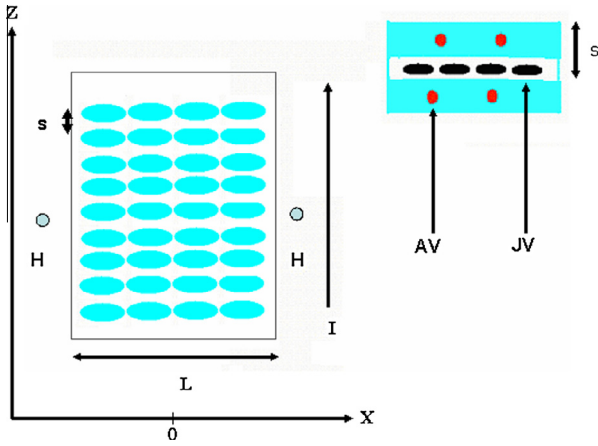*E-mail address:* shapib@mail.biu.ac.il (B.Ya. Shapiro).

Fig. 1. The model system – layers of superconducting materials with periodicity s in the z-direction, subjected to an external magnetic field, H, along the y-direction, carrying a bias current, J, in the z-direction. The Josephson channels are along the x-direction. Inset: zooming on two adjacent grains forming an extended Josephson junction. Voltage is induced by motion of both Josephson vortices (black ellipsoids) and unpinned Abrikosov vortices (red dots).

Fig. 2. Magnetic induction across a Josephson channel for $\eta = 0.5$, and $\alpha = 0.27$. Lowest curve: $h = 1.56$, just below the Josephson critical field; middle and upper curves, respectively: $h = 1.6$ and $h = 4$, demonstrating soliton-like and large wave amplitude distribution.

the induction B_n in the n-th junction to the phase difference ϕ_n between the grains on both sides of the junctions reads [5–8]:

$$\frac{c}{4\pi J_c}\frac{\partial B_n}{\partial x} - \frac{1}{\omega_p^2}\frac{\partial^2 \varphi_n}{\partial t^2} - \frac{\sigma_{zn}(B_n)\phi_0}{2\pi c s J_c}\frac{\partial \varphi_n}{\partial t} = \alpha + \sin\varphi_n, \quad (1)$$

where $\alpha = J/J_c$, J is the bias current density, $J_c = \frac{c\phi_0}{8\pi^2 s \lambda_z^2}$ is the Josephson critical current density, $\omega_p = \frac{c}{\lambda_z \sqrt{\varepsilon_z}}$, s is the periodicity of the layers, $\sigma_{zn}(B_n)$ is the magnetic-field dependent conductivity of the quasi-particles across the contact, in the z-direction, ε_z is the dielectric constant. In the general case, the magnetic induction B_n is affected by the induction in neighboring channels:

$$B_n = \frac{\phi_0}{2\pi s}\frac{\partial \varphi_n}{\partial x} - \frac{\lambda_{xy}^2}{s^2}(B_{n+1} + B_{n-1} - 2B_n).$$

Note that the third term in the left hand side of Eq. (1) couples the JV dynamics with the normal electrons. Eq. (1) has to be completed by the boundary conditions: $B_n = H_{ext}$ at $x = \pm L/2$ (see Fig. 1). Solution of Eq. (1) allows calculation of the voltage V_n generated along the n-th channel using the conventional Josephson equation:

$$V_n = \frac{\phi_0}{2\pi c}\frac{\partial \varphi_n}{\partial t} \quad (2)$$

Assuming that the magnetic field in a channel is only slightly affected by the currents in neighboring channels, the index n can be ignored and Eq. (1) may be written in dimensionless units as:

$$\frac{\partial^2 \varphi}{\partial X^2} - \frac{\partial^2 \varphi}{\partial \tau^2} - \eta(T,b)\frac{\partial \varphi}{\partial \tau} = \sin\varphi + \alpha \quad (3)$$

where

$$X = x/\lambda_J; \quad \tau = t\omega_p; \quad b = \frac{\partial \varphi}{\partial X} = B_n/H_J;$$
$$H_J = \phi_0/2\pi\gamma s^2; \quad \eta = \frac{\sigma_{zn}(B_n)\omega_p\phi_0}{2\pi c s J_c}.$$

Here, $\lambda_J = \gamma s$ is the Josephson penetration length.

In these dimensionless units, the voltage induced by the JV dynamics, measured in units of $\hbar\omega_p/2e$, is given by

$$V_J = \lim_{T \to \infty}\frac{N}{T}\frac{\hbar}{2e}\int_0^T \frac{\partial \varphi}{\partial t}dt \quad (4)$$

where N is the number of Josephson channels along the z-direction.

Fig. 2 shows numerical solutions of Eq. (3) for $\eta = 0.5$, utilizing the Crank–Nicholson algorithm [9]. Qualitatively, similar solutions
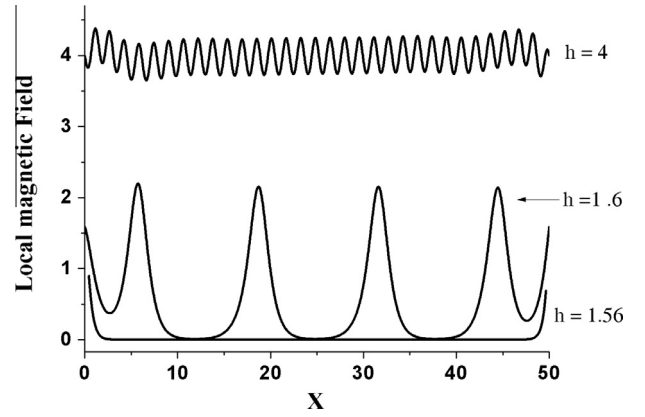
are obtained for η in the range 0.5–50. For small magnetic fields, up to $h = H_{ext}/H_J \sim 1.57$ (the Josephson critical field), a complete screening of the field is obtained (lowest curve in Fig. 2). As h increases above the critical field, the spatial distribution of the JV magnetic-induction along the junction is soliton-like, very similar to that in dissipation-less Josephson junctions (middle curve in Fig. 2). As the field further increases, this behavior transforms into dense "large amplitude waves" (upper most curve in Fig. 2, see also Ref. [10]). (The number of JV is limited, of course, by the length of the junction taken as 50 λ_J in the figure). The crossover field from a soliton-like solution to the large amplitude waves regime is around $h = 2$, independent of temperature.

To explain the experimentally observed negative magnetoresistance slope we assume a linear dependence of the conductivity on the induction: $\sigma_{zn}(B_n) = \sigma_0(1 + \varepsilon(T)B_n/H_J)$. This is justified by the linear increase in the number of quasi-particles with the field due to the increase in the number of AV in the grains. The induction is normalized to H_J as this field is of order of the Josephson critical field; around this field the magnetic field penetrates the inter-grains space and Abrikosov vortices nucleate inside the grains, resulting in creation of quasi-particles localized at the vortex cores. The pre-factor σ_0 defines the remnant inter-grain conductivity at $T = 0$, i.e. the conductivity governed by electron-impurities scattering conductivity. The temperature dependence of the conductivity is assumed to originate from the electron–phonon part of the conductivity, σ_{e-ph}. Thus, $\varepsilon(T) = \sigma_{e-ph}/\sigma_0 = \tau_{e-ph}/\tau_{imp}$, where τ_{e-ph} and τ_{imp} are the electron-phonon and the electron-impurities scattering times of the inter-grain quasi-particles, respectively. Using the Bloch relation $\tau_{e-ph} = \omega_D^4(\hbar/T)^5$ and the Drude approximation $\sigma_0 = (ne^2/m)\tau_{imp}$ for the remnant inter-grain conductivity, one obtains $\varepsilon(T) \propto T^{-5}$ (Bloch law) [11].

The dimensionless viscosity, η in Eq. (4) can now be expressed as follows:

$$\eta(T,b) = a(1 + \varepsilon(T)b) \quad (5)$$

where $a = 4\pi\sigma_0\omega_p\lambda_z^2/c^2$. Note that $\varepsilon(T)b$ is proportional to the number of quasi particles.

Numerical solution of Eq. (3) for the time dependence of ϕ allows calculation of the voltage using Eq. (4). This voltage, induced by the moving JV, is presented in Fig. 3 for different values of the parameter ε as a function of the external magnetic field normalized to H_J. The voltage is zero up to the critical Josephson induction $\sim 1.57 H_J$. Above this field, initially the voltage increases rapidly as the field increases, reflecting dissipation due to motion of the JV. As the field is further increased the effect of the field on the
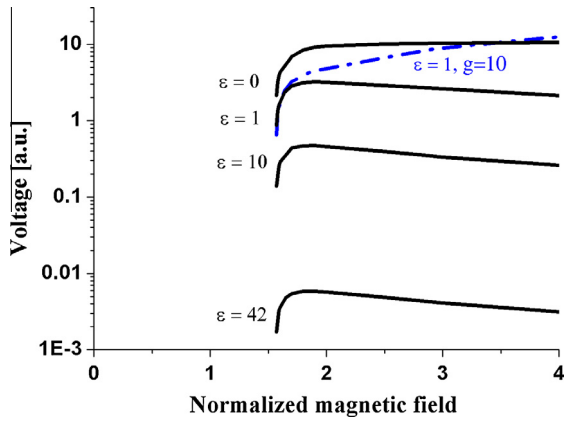
Fig. 3. Solid curves: calculated voltage in arbitrary units *versus* external magnetic field normalized to H_J for different values of the parameter ε taking the normalized current $\alpha = 0.27$ and $a = 0.5$. The solid lines correspond to $g = 0$. The dashed curve is calculated for $\varepsilon = 1, g = 10$. (For interpretation of the references to colour in this figure legend, the reader is referred to the web version of this article.)

Fig. 4. Voltage *versus* magnetic field measured in a granular YBCO bridge at the indicated temperatures. The slope of the magnetoresistance at high fields decreases as temperature is lowered and eventually changes sign, exhibiting a *negative* magnetoresistance slope at low temperature. The solid (blue) lines are calculated from Eqs. (3) and (4) using the parameters $(\varepsilon, g) = (42, 0), (10, 0), (3.2, 9 \times 10^{-5})$ and $(1, 3.5 \times 10^{-4})$ for the 30, 40, 50 and 60 K, respectively.

dissipation is more moderate due to the highly dense JV matter. This is demonstrated by the $\varepsilon = 0$ curve (i.e. for σ and η independent of the field) which exhibits a slope of approximately zero above approximately $h = H_{ext}/H_J = 2$. Note that this field signifies also the crossover from soliton-like spatial distribution of the induction into large amplitude waves (Fig. 2). As ε increases (temperature decreases), a negative slope sets in around the same field. Remarkably, the onset of the negative slope is independent of the value of ε, i.e. independent of temperature. The origin of the negative slope for $\varepsilon \neq 0$ can be traced to the (linear) increase in the number of quasiparticles with the magnetic field. Quasiparticles localized in the vortex cores contribute to the tunneling conductivity and hence reduce the resistance of the junction.

So far we neglected dissipation due to the motion of intra-grains Abrikosov vortices. This is justified at low temperatures where the vortices are pinned. At high temperatures, however, the Abrikosov vortices are depinned and their motion can dominate the voltage generation. We approximate the voltage in this temperature range by the Bardeen–Stephen model [12]:

$$V_A = gB/H_J = gb, \qquad (6)$$

where $g = \frac{R_N IH_J/H_{c2}}{\hbar \omega_p/2e}$. Neglecting the interaction between the AV and the JV, the total voltage produced by the motion of both JV and AV is given by $V_t = V_J + V_A$. In Fig. 3 we also plot V_t in arbitrary units using $\varepsilon = 1$ and $g = 10$. Apparently, the slope of the voltage is now positive due to the motion of AV.

3. Comparison with experimental results

In the following we compare the theoretical predictions outlined above with our experimental results obtained in granular ultra-thin YBCO bridges [4]. Obviously, we do not expect to obtain quantitative agreement as our system is much more complicated than the theoretical model. Nevertheless, as we show below, qualitative comparison yields reasonable agreement. As an example we shown in Fig. 4 data obtained for a $700 \times 500 \times 10\ nm^3$ YBCO bridge. (For details of sample preparation and measurements, see Refs. [4,13].) The magnetoresistance exhibits oscillations, resulting from phase coherent loops [14], superimposed on a field-dependent background. This magnetoresistance background, which is the subject of the present paper, exhibits clearly two distinct behaviors at low and high temperatures. While at high temperature the background increases monotonically with field, at low
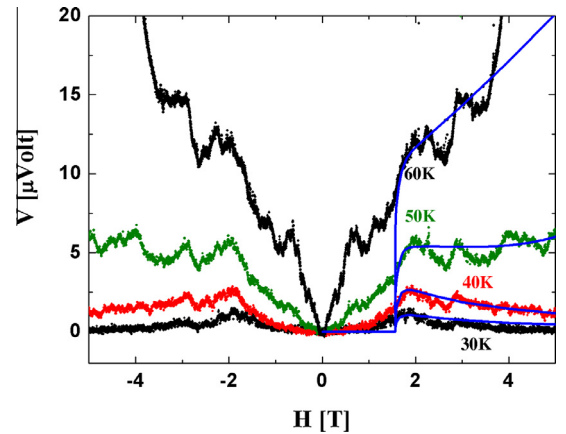
temperatures it exhibits a peak around 2 T independent of temperature. According to the analysis outlined above, this field should correspond to $2H_J$, allowing scaling of the theoretical field-axis to the experimental one. The experimentally measured value of $H_J = \phi_0/2\pi\gamma s^2 \approx 1\ T$ yields $\gamma s^2 \approx 3 \cdot 10^{-12}$. Assuming that the anisotropy parameter $\gamma = 1–10$ we find s between 5 and 17 nm. As the measured average size of the grains in this sample is ~ 50 nm, the values derived for s suggest that only small grains contribute to the negative slope. According to this scenario, the contribution of the larger grains is saturated at high fields.

The parameter $\varepsilon = \tau_{e-ph}/\tau_{imp}$ can be estimated as follows. Estimating the Fermi velocity $v_F = 10^7\ cm/s$ and the electrons mean free path $\ell = 10^{-6}\ cm$ [16], one obtains $\tau_{imp} \sim \ell/v_F \simeq 10^{-13}s$. The electron-phonon scattering time is estimated as $\tau_{e-ph} \sim 10^{-12}s$ [15], yielding $\varepsilon = 10$. We adopt this value for $T = 40$ K. The parameter ε for the other temperatures was calculated using the Bloch law, $\varepsilon(T) \propto T^{-5}$, yielding $\varepsilon = 42, 3.2$ and 1 for 30, 50 and 60 K, respectively.

The solid lines through the 40 K and 30 K data in Fig. 4 were calculated for $\varepsilon = 10$ and 42, neglecting the contribution of the AV to the voltage (i.e., $g = 0$) and normalizing the calculated voltage to the peak value of the measured voltage. Apparently, the calculated lines capture the salient features of the data, namely, the negative slope and its onset at the same field, independent of temperature. Good qualitative agreement of the high field data is also obtained for the 50 K and 60 K data after adding the contribution of AV, taking the fitting parameter in Eq. (5), $g = 9 \times 10^{-5}$ and 3.5×10^{-4} for the 50 and 60 K data, respectively. These values of g reasonably agree with the following estimate: $\lambda_z = 100$ nm and $\sqrt{\varepsilon_z} = 1$ yield $\omega_p = \frac{c}{\lambda_z\sqrt{\varepsilon_z}} = 3 \times 10^{15}s^{-1}$. From the experiment we get $H_J/H_{c2} \approx 0.01$ and $R_N I \approx 2 \times 10^{-3}$ V [4], yielding $g \approx 10^{-5}$. As temperature decreases H_{c2} increases and, consequently, g decreases.

Apparently, the calculated lines in Fig. 4 show zero voltage at low fields below $1.57H_J$, the critical field for flux entry into the junctions. However, we note that the theory outlined above does not take into account phase slips that may also contribute to the voltage. The voltage measured at low fields may be attributed to phase slips in weak junctions – a contribution which saturates at high fields.

Finally, we note that the theory outlined above may also explain qualitatively the disappearance of the negative slope for large bias currents as described in Fig. 4 of Ref. [4]. It is clear from Eq. (5) that as the bias current increases the contribution of the AV motion increases, and it can overcome the negative contribution of V_J.

4. Summary

The sine-Gordon equation describing the temporal and spatial dependence of the phase in a Josephson junction is extended to include a viscosity term that increases linearly with the external field. This term arises from the increase in the number of quasi-particles because of the increase in the number of vortices as the field increases. Including such a term yields a negative magnetoresistance slope setting in around the field for which a soliton-like behavior of the induction in the junction crosses over to the large amplitude wave's regime. This field is determined by the geometry and, therefore, it is independent of temperature. This behavior characterizes the magnetoresistance at low temperature where the contribution of the Abrikosov vortices to the voltage may be neglected. Including this contribution may change the magnetoresistance slope to zero and even positive values. These results capture the salient features of experimental magnetoresistance data in YBCO granular bridges, although the experimental system is much more complex than the model system.

Acknowledgements

References

[1] N. Morozov, L. Krusin-Elbaum, T. Shibauchi, L.N. Bulaevskii, M.P. Maley, Y.I. Latyshev, T. Yamashita, Phys. Rev. Lett. 84 (2000) 1784.
[2] L.N. Bulaevskii, D. Domínguez, M.P. Maley, A.R. Bishop, B.I. Ivlev, Phys. Rev. B 53 (1996) 14601.
[3] R. Córdoba, T.I. Baturina, J. Sesé, A. Yu Mironov, J.M. De Teresa, M.R. Ibarra, D.A. Nasimov, A.K. Gutakovskii, A.V. Latyshev, I. Guillamón, H. Suderow, S. Vieira, M.R. Baklanov, J.J. Palacios, V.M. Vinokur, Nat. Commun. 4 (2013) 1437.
[4] D. Levi, A. Shaulov, G. Koren, Y. Yeshurun, Phys. C: Supercond. 495 (2013) 39.
[5] L. Bulaevskii, J.R. Clem, Phys. Rev. B 44 (1991) 10234.
[6] S.N. Artemenko, S.V. Remizov, JETP Lett. 66 (1997) 853.
[7] A.E. Koshelev, Phys. Rev. B 76 (2007) 054525.
[8] G.R. Berdiyorov, A.R. Romaguera, M.V. Milošević, M.M. Doria, L. Covaci, F.M. Peeters, Eur. Phys. J. B 85 (2012) 1.
[9] J. Crank, P. Nicolson, Proc. Camb. Philos. Soc. 43 (1947) 1.
[10] A. Barone, G. Paterno, Physics and Applications of the Josephson Effect, John Wiley & Sons, New York, 1982 (Chapter 13.2).
[11] F. Bloch, Zeitschrift Phys. 59 (1930) 208;
A.A. Abrikosov, Introduction to the Theory of Normal Metals, Academic Press Inc., 1972.
[12] J. Bardeen, M.J. Stephen, Phys. Rev. 140 (1965) 972.
[13] D. Levi, A. Shaulov, A. Frydman, G. Koren, B.Y. Shapiro, Y. Yeshurun, EPL (Europhysics Letters) 101 (2013) 67005.
[14] A.V. Herzog, P. Xiong, R.C. Dynes, Phys. Rev. B 58 (1998) 14199.
[15] M. Lindgren, M. Currie, C. Williams, T.Y. Hsiang, P.M. Fauchet, R. Sobolewski, S.H. Moffat, R.A. Hughes, J.S. Preston, F.A. Hegmann, Appl. Phys. Lett. 74 (1999) 853.
[16] D.M. Ginsberg (Ed.), Physical Properties of High Temperature Superconductors, vol. 1, World Scientific London, 1989.